

# Computer-Assisted Nonlinear Regression Analysis of the Multicomponent Glucose Uptake Kinetics of *Saccharomyces cerevisiae*

DAVID M. COONS,<sup>1</sup> ROGER B. BOULTON,<sup>1,2</sup> AND LINDA F. BISSON<sup>1\*</sup>

*Department of Viticulture and Enology, University of California, Davis, California 95616-8749,<sup>1</sup> and Department of Chemical Engineering and Materials Science, University of California, Davis, California 95616-5924*

Received 6 October 1994/Accepted 30 March 1995

**The kinetics of glucose uptake in *Saccharomyces cerevisiae* are complex. An Eadie-Hofstee (rate of uptake versus rate of uptake over substrate concentration) plot of glucose uptake shows a nonlinear form typical of a multicomponent system. The nature of the constituent components is a subject of debate. It has recently been suggested that this nonlinearity is due to either a single saturable component together with free diffusion of glucose or a single constitutive component with a variable  $K_m$ , rather than the action of multiple hexose transporters. Genetic data support the existence of a family of differentially regulated glucose transporters, encoded by the *HXT* genes. In this work, kinetic expressions and nonlinear regression analysis, based on an improved zero *trans*-influx assay, were used to address the nature of the components of the transport system. The results indicate that neither one component with free diffusion nor a single permease with a variable  $K_m$  can explain the observed uptake rates. Results of uptake experiments, including the use of putative alternative substrates as inhibitory compounds, support the model derived from genetic analyses of a multicomponent system with at least two components, one a high-affinity carrier and the other a low-affinity carrier. This approach was extended to characterize the activity of the SNF3 protein and identify its role in the depression of high-affinity uptake. The kinetic data support a role of SNF3 as a regulatory protein that may not itself be a transporter.**

There has been a great deal of discussion regarding the current understanding of glucose uptake kinetics in the yeast *Saccharomyces cerevisiae*. This discussion includes questions as to the number and characteristics of distinct protein-mediated systems and the role of the putative transport proteins, encoded by the *SNF3* and *HXT* genes, in these processes (3, 12–15, 19, 21, 35, 39).

*S. cerevisiae* is capable of utilizing sugar concentrations varying over 3 orders of magnitude, from the millimolar to the molar ranges (3). An Eadie-Hofstee {rate of uptake ( $v$ ) versus  $v$  over substrate concentration ( $[S]$ )} plot of glucose uptake in *S. cerevisiae* is a nonlinear diagnostic of multicomponent uptake. The high-affinity portion of the graph displays a significant level of glucose repressibility (1, 2). The nonlinear plot has been described as resulting from a multiple-protein mediated system with a high-affinity component with an apparent  $K_m$  of approximately 2 mM and a low-affinity component with an apparent  $K_m$  of approximately 20 mM (1–7). It has recently been described as resulting from a combination of carrier-mediated transport and free diffusion, with the saturable component having a  $K_m$  ranging from approximately 1 to 6 mM and the nonsaturable component having a  $K_d$  ranging from approximately 0.8 to 1.3  $\mu\text{g mg}^{-1} \text{min}^{-1}$  (12–14, 39), or, alternatively, as a result of differential regulation of a single system with affinities changing with growth condition (35).

Genetic, physiological, and biochemical evaluation of glucose uptake in *S. cerevisiae* has shown that the process is a complex one involving many gene products. Several lines of evidence implicate the *HXT* family of proteins, which are part of a sugar transporter superfamily (3, 16), as glucose transport-

ers in *S. cerevisiae*. Deletion of either the *HXT1* or *HXT2* gene results in a reduced level of high-affinity glucose upon a shift to conditions under which these proteins are expressed (7, 20, 23, 36, 37). Overexpression of *HXT1* (23), *HXT2* (20), or *HXT4* (33) results in elevated levels of glucose transport activity. Overexpression of the *HXT3* gene also suppresses the *snf3* growth defect in the presence of low glucose concentrations and may confer an increased-transport phenotype as well (19). Low- and medium-stringency Southern blotting using an *HXT2*-based probe indicate there may be other homologous, as yet unidentified *HXT* genes in the *S. cerevisiae* genome (20). Indeed, six additional *HXT* genes (*HXT5* to *HXT10*) have been discovered as a consequence of the yeast genome sequencing project. Genetic data do not, therefore, support a claim of a single glucose transporter.

The *HXT* genes do not appear to be expressed constitutively. The *HXT2* protein has been shown to be regulated by glucose concentration at the transcriptional level (30, 37), by turnover (36), and possibly by posttranslational modification (37). *HXT1* (23), *HXT3* (29), *HXT4* (33), and *SNF3* (9) are also glucose responsive. None of these putative transporters is constitutive. Such responses to changing glucose concentrations in the media involve regulation by the cyclic AMP-dependent, the RAS adenylate cyclase, and possibly the inositol-phosphate cascades (3). Finally, chimeric proteins constructed between *GAL2* and *HXT2* were used to define the galactose recognition domain (28). This study confirms the role of *HXT2* as a transporter in that its substrate specificity was altered upon introduction of the galactose recognition domain (28). Therefore, the *HXT* proteins appear to be bona fide glucose transporters. These observations strongly suggest that the observed kinetics of glucose transport result from multiple contributing factors that change in response to a complex regulatory cascade.

\* Corresponding author. Phone: (916) 752-8035. Fax: (916) 752-0382.

Previous kinetic modeling of glucose transport has yielded conclusions incompatible with data generated on the numbers and regulation of the *HXT* genes. We undertook our own kinetic analysis to determine the basis of the apparent conflict in these two sets of data. The method of nonlinear regression allows analysis of complex processes such as substrate transport (22). By using a mathematical description of an enzymatic process, we can statistically evaluate how well a kinetic model describes a set of experimental data. Especially when used in conjunction with genetic or biochemical data, this analysis can significantly further our understanding of these kinetically complex systems.

While this technique is useful for analyzing kinetic data, it does have limitations. In a system with multiple components catalyzing the same reaction, no more than two independent components can be discerned reliably by using computer-assisted nonlinear regression (17, 18). Although this modeling approach is limited to a two-component system, it can be used to differentiate between a two-carrier model and models calling for either a carrier with a nonsaturable (diffusion) component or a regulated carrier with varying affinity. It can also be used, in conjunction with genetic data, to test certain specific questions regarding the degree of contribution of certain proteins to this process.

Facilitated diffusion processes display complex kinetics (reviewed in references 34 and 38). Both loaded and unloaded carriers can traverse the membrane. These transporters display the kinetic phenomena of influx (entry), efflux (exit), and exchange (a swap of substrate in either direction). The exchange phenomenon is strikingly indicative of a facilitated diffusion process and cannot be explained by simple diffusion. Glucose transport in yeast cells displays these same kinetic complexities (8, 10). Early researchers in the field recognized the difficulties in design of uptake assays that arise as a consequence of the kinetic behavior of facilitated diffusion transporters (31). The transport assay originally described (4) was based on previous work in the field of transporter analysis (10, 30). Carrier movement is terminated at the end of the substrate incubation period by addition of ice-cold buffer (4). Several studies demonstrated the dramatic temperature sensitivity of carrier function (31). Net efflux or influx can effectively be stopped by rapid imposition of low temperature in a manner that does not disrupt plasma membrane structure. However, the exchange reaction appears to be less temperature sensitive. It is thought that the temperature-sensitive step is substrate dissociation from the carrier. In the case of exchange, one substrate molecule displaces another from the binding site. Therefore, inclusion of a high-substrate wash, which has recently been recommended (35), may generate a potential artifact due to the exchange reaction.

The previously described zero *trans*-influx assay (4) was subject to experimental error resulting primarily from low signal-to-noise ratios, especially at high substrate concentrations. This assay produces data that are valuable as an indication of trends and magnitudes, as reviewed in reference 22, but are not of the rigor required for detailed mathematical analysis. Thus, nonlinear regression analysis of such data, especially in the low-affinity range, should be critically viewed (12–14, 39). Improvements in the uptake assay protocol used for this study resolve these problems of low signal-to-noise ratios and give reproducible results that are of sufficient quality to provide a strong basis for computer modeling. The data presented contain a margin of error (expressed as a standard deviation from the mean) of no greater than 10% of the total rate for a given point. The margin of error is generally much lower, but be-

cause of low signal-to-noise ratios at high substrate concentrations, the error occasionally approaches 10% in that range.

As mentioned above, the range of sugar concentrations that can be transported by *S. cerevisiae* spans 3 orders of magnitude, and the contributing systems differ in apparent affinity for glucose at least by a factor of 10. When one is examining a system with significant activity over such a broad range, it is important to weight the extremes of concentration equally to obtain a reliable assessment of contributing factors (22). The functional form used to analyze the data will dramatically affect the values of the constants generated in a regression analysis. Regression analysis using only a Michaelis-Menten plot of the data effectively provides more weight to the portion of the curve resulting primarily from the low-affinity component of transport. Analysis using a the Lineweaver-Burk form will result in a similar emphasis of the high-affinity component. These transformations can result in an underestimation of the number of contributing systems (see Fig. 2). In this report, we address this issue by using two functional forms, the Michaelis-Menten ( $v$  versus  $[S]$ ) and the Lineweaver-Burk (a double-reciprocal plot,  $1/v$  versus  $1/[S]$ ) forms, in an iterative computation procedure to determine the kinetic parameters and account for the different contributions. It should be noted that in this approach, the kinetic parameters are not necessarily the best fit for any single functional form but rather the best overall fit for both forms of a data set. The data are also presented in the Eadie-Hofstee ( $v$  versus  $v/[S]$ ) form to aid in comparison to previous publications. Because error is present on both axes, the Eadie-Hofstee plot is not useful in regression analysis, which assumes error on a single axis (22).

## MATERIALS AND METHODS

**Reagents.** All reagents, unless otherwise noted, were obtained from Fisher Scientific and were reagent grade. L-Glucose was purchased from Sigma; ACS reagent-grade D-glucose used in the uptake assays was purchased from Aldrich. Medium components were obtained from Difco. D- $^{14}$ C]glucose and L- $^3$ H]glucose were purchased from Amersham Life Sciences.

**Yeast strains.** The *S. cerevisiae* strains used in this study were YPH500 and YPH499, which have been described previously (32), and LB312 (*MAT $\alpha$  snf3 $\Delta$ ::TRP1 ura3-52 lys2-801<sup>amber</sup> ade2-100<sup>ochre</sup> trp1- $\Delta$ 63 his3 $\Delta$ 200 leu2 $\Delta$ 1 mel SUC2*). LB312 was constructed by integration of the *snf3 $\Delta$ ::TRP1*-containing *SalI-EcoRI* fragment from plasmid pSNF3::TRP1 into the genome of YPH500 at the *SNF3* locus. pSNF3::TRP1 was constructed by insertion of the *TRP1*-containing *BglII-NcoI* fragment of pG-N795 (29) into *BamHI-BglII* sites of the disrupted *snf3* gene in plasmid pSNF3.R. pSNF3.R was constructed by insertion of the *SNF3*-containing *SalI* fragment from the YCp50-based plasmid pSC4 (27) into the *SalI* site of the plasmid pUN75 (11). The resultant strain was backcrossed three times into the parental background. LB312 was crossed with LB312 (20) and checked for correct insertion location by segregation analysis. All strains are congenic to S288C.

**Culture conditions.** Strains were grown in 500 ml of YE2% (1% yeast extract, 2% Bacto Peptone, 2% glucose) overnight to mid-logarithmic growth phase. Cultures were then harvested by centrifugation at 2,000  $\times$  g at 4°C for 5 min in a Sorvall GSA rotor. The supernatant was decanted, and the cell pellet was resuspended in either YE2% or YE0.05% (1% yeast extract, 2% Bacto Peptone, 0.05% glucose), as dictated by the experimental parameters. Cells were then cultured for an additional 2 h before collection for use in uptake assays.

**Preparation of labeled sugar substrates.** Labeled glucose was purchased as an ethanol solution, divided into three equal portions, and dried *in vacuo*. The resultant crystalline radiolabeled glucose was dissolved in a glucose solution that resulted in a final concentration of either 1 M, 100 mM, or 10 mM at a specific activity of approximately 250,000 dpm/ $\mu$ l.

**Zero *trans*-influx assays.** In order for the uptake data generated in the zero *trans*-influx assay to be of sufficient accuracy for computer-assisted nonlinear regression analysis, several changes were made in the standard protocol for this procedure (4, 20). It was found that the use of glass-fiber filters resulted in high backgrounds, especially at the higher substrate concentrations. Further, an assay consisting of only 10 substrate concentrations covering a substrate range differing by 2 orders of magnitude, while adequate for detecting general trends and magnitudes, does not contain enough data points or experimental determinations for satisfactory computer modeling.

These problems were addressed in a number of ways. Use of nylon filters that show low nonspecific binding of labeled glucose during cell collection signifi-

cantly reduced filter-related background. The protocol used 25-mm-diameter, 5- $\mu\text{m}$ -pore-size filters (MSI catalog no. N50SP02500) and a Hoefer model FH125 filter head. The large pore size and special filter head were used to maximize flowthrough rate. There were no detectable yeast cells in the filtrate that was collected, centrifuged, and examined microscopically for particulates. This protocol uses a 10-s uptake period, twice that of the previously described method (4). This was tested and found to be in the linear range of glucose uptake at the concentrations tested and allows a greater signal-to-noise ratio. Because nonspecific background problems seem to result primarily from interaction of the labeled sugar with the filter matrix rather than the cell surface, it was possible to increase the signal-to-noise ratio by the addition of more cells to the assay. This was done by doubling the volume and the density of cell suspension that was added to the reaction mixture. All assays were monitored so that no more than 5% of the substrate was depleted. Because of the increase in assay time, it was necessary to store aliquots of cell suspension on ice until they were needed, in order to prevent physiologic changes resulting from prolonged incubation in a buffer solution at 30°C. Cells that are stored in this fashion for up to 3 h and then equilibrated at 30°C are kinetically indistinguishable from fresh cells at the concentrations tested. The protocol described below is the result of these changes.

In quintuplicate, 10 ml of cells cultured as described above is filtered through tared 25-mm-diameter, 1.2- $\mu\text{m}$ -pore-size nylon filters (MSI catalog no. N12SP02500), washed with 10 ml of 100 mM potassium phosphate buffer (pH 6.8), dried for 18 h at 50°C in a vacuum oven, and weighed, and the results are averaged to determine cell dry weight. A culture volume sufficient to yield 15 ml of a cell suspension with an optical density at 580 nm of approximately 25 is collected by filtering through a 47-mm-diameter, 0.45- $\mu\text{m}$ -pore-size nylon filter (MSI catalog no. E04WG047S1) and is washed three times with 10 ml of 100 mM potassium phosphate buffer (pH 6.8). These cells are then suspended in 15 ml of 100 mM potassium phosphate buffer (pH 6.8) and divided into five aliquots of 3 ml each. Four of these are placed on ice, and one is placed in a water bath at 30°C to equilibrate for 2 min. The actual optical density at 580 nm of the cell suspension is checked by measuring a 1:100 dilution.

There are 19 different substrate concentrations tested at 21 different assay points. Each point is tested in duplicate, and each experiment is repeated for a total of four data points for each experimental concentration. One hundred sixty microliters of cell suspension is added to 40  $\mu\text{l}$  of labeled sugar, for a total assay volume of 200  $\mu\text{l}$ . The 1 M stock solution, diluted with deionized water as necessary, is used to generate glucose concentrations which will result in final substrate concentrations, after addition of the cell suspension, of 200, 150, 100, 75, 50, 35, and 20 mM. The 100 mM stock is similarly used to generate concentrations of 20, 15, 10, 7.5, 5, 3.5, and 2 mM, and the 10 mM stock is used to generate concentrations of 2, 1.5, 1, 0.75, 0.5, 0.35, and 0.2 mM.

Uptake activity at each concentration is determined at 0 and 10 s. For the 10-s time point, the cell suspension is added, using a pipettor, and mixed with the labeled sugar. The reaction is quenched by the addition of 10 ml of 0°C deionized water delivered by a syringe with sufficient pressure to disperse the suspension thoroughly. The 0-s time point is handled analogously, but the quenching water is added simultaneously with the cell suspension. It is critical that this addition be simultaneous. Addition of the cells to diluted label reduces surface binding and overestimates uptake. A delay in cold-stop of the zero point results in an underestimation of uptake. The resultant suspension is filtered through a 5- $\mu\text{m}$ -pore-size 25-mm-diameter nylon filter (presoaked in 40% glucose) and washed twice with 10 ml of 0°C deionized water. The filter is then placed in a 20-ml borosilicate liquid scintillation vial containing 5 ml of Packard Optifluor scintillation cocktail.

The aliquots of cell suspension were used sequentially. No cell suspension was allowed to be at 30°C for more than 20 min, and each sample that was taken from ice was allowed to equilibrate for 5 min prior to use. The incorporated radioactivity was measured with a Packard 2000 Tri-Carb liquid scintillation counter over a range of 0 to 156 keV, and the data are reported as decays per minute. While this assay resulted in greatly reduced error, necessary for modeling studies, we found that the results are in good general agreement with those generated by using the previously described assay (4).

**Inhibition studies.** Experiments to determine the inhibition kinetics of fructose and 2-deoxyglucose (2-DOG) were done as described above except that 20  $\mu\text{l}$  of inhibitor solution was added to the labeled sugar solution to a concentration sufficient to result in the experimental inhibitor concentration. This increase in volume was compensated for by reducing the volume of the added cell suspension to 140  $\mu\text{l}$  and increasing the density of that suspension so that the amount of cells added was the same.

**Time course experiments.** The accumulation of internal radioactivity was used as a measure of uptake. A series of tubes was prepared with labeled sugar at the concentration noted for each experiment. A zero time point was subtracted from all subsequent time points. Samples were taken sequentially at the times noted and were handled and analyzed as described above.

**Modeling and statistical analysis.** Computer modeling of the uptake data was done by using Island Product's NFIT curve-fitting program, version 1.0, run on an Intel 486-33 personal computer. As it is not possible to directly model an Eadie-Hofstee plot of a two-carrier system with this algorithm, modeling was done by using both Michaelis-Menten and Lineweaver-Burk plots. The kinetic constants given represent the parameters that best describe both the Michaelis-

Menten and double-reciprocal plots, not necessarily the best fit for either plot singly. Michaelis-Menten plots were described in the standard form:

$$v = (V_{\max 1}[S])/(K_{m1} + [S]) + (V_{\max 2}[S])/(K_{m2} + [S]) \quad (1)$$

and Lineweaver-Burk plots were described as

$$1/v = ((K_{m1} + [S])(K_{m2} + [S])) / (V_{\max 1}K_{m2} + V_{\max 1}[S] + V_{\max 2}[S] + V_{\max 2}K_{m1})(1/[S]) \quad (2)$$

By using the starting parameters of  $V_{\max 1} = 80$ ,  $K_{m1} = 20$ ,  $V_{\max 2} = 8$ ,  $K_{m2} = 2$ , NFIT was used to perform parameter estimation in the Michaelis-Menten form. The resulting values were then used as starting parameters, with the low-affinity values held as constants, to determine the parameters of the Lineweaver-Burk form. The high-affinity constants derived in this way were then used to refine the accuracy of the low-affinity values in a Michaelis-Menten regression. This process was repeated until the  $\chi^2$  values were changing by less than 0.5% between iterations. This entire process was repeated, starting with the Lineweaver-Burk form, and the resulting values were compared with those generated by the first approach. If there were discrepancies between the two results, the constants reflecting the best fit are reported.

Inhibition studies were modeled by using the technique described above.  $K_i$  values were not determined. While estimations of the constants which describe the experimental data with a high degree of correlation can be derived, the validity of these constants is questionable because of the complexity of the iteration and the limitations of the regression analysis algorithm. Thus, we only attempt to access the degree of inhibition by comparison of the kinetic constants in the presence of inhibitor with the uninhibited values.

The model of single-carrier- and free-diffusion-mediated transport was tested by using the following equation:

$$v = V_{\max}([S])/(K_m + [S]) + K_d[S] \quad (3)$$

Initial values were set at zero, and the parameters were estimated by using the program NFIT.

All values are reported to two decimal places. This does not indicate that the values are accurate to that degree. The values were generated by regression analysis of experimental data, which involves a margin of error. Further, as discussed earlier, these results do not preclude the possibility of a more complex kinetic model. These values are given to describe the best fit of the simplest model that adequately describes the data and are given to a degree of precision that allows other researchers to check our results.

## RESULTS

**Free diffusion of hexose across the yeast plasma membrane is not sufficient to account for the observed kinetics.** L-Glucose is a stereoisomer of D-glucose, and any nonstereospecific reactions such as simple diffusion will affect both compounds equally. Thus, if a significant amount of D-glucose uptake is mediated by free diffusion, then a comparable amount of uptake of L-glucose ought to be observed. Such a contribution can then be subtracted from a kinetic plot of D-glucose uptake in *S. cerevisiae*, and the remaining portion would reflect carrier-mediated uptake. Previously published work (4) indicated that L-glucose is not transported efficiently by *Saccharomyces* cells. Since the assay protocol has been modified in this study, the kinetics of uptake of L-glucose were reevaluated.

YPH500 was grown to mid-log phase in YEPD<sub>2%</sub> and then shifted to repressing conditions for 2 h. The uptake of 100 mM L-[<sup>3</sup>H]glucose was then measured over a period spanning 20 min (Fig. 1). The rate of accumulation was found to occur at an average value of 0.342 nmol mg<sup>-1</sup> min<sup>-1</sup>. The 20-minute assay was necessitated by the extremely low rates of uptake and the need to average over time in order to generate a reliable slope from which to calculate an approximate rate. Comparison of this slope with that for the 10-s rate of D-glucose uptake in cells prepared and handled analogously shows that D-glucose is accumulated about 150 times more rapidly. This result shows that free diffusion makes a negligible contribution to glucose uptake in *S. cerevisiae* and can effectively be ignored in kinetic modeling. It should also be noted that this result demonstrates that the contribution of nonspecific binding of labeled sugar to the cell to uptake rates is negligible when this protocol is used.

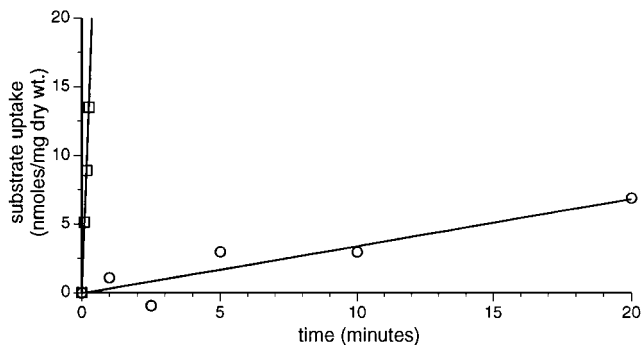


FIG. 1. Uptake of L-glucose. The uptake of 100 mM L-glucose was monitored for 20 min, and the rate of uptake was determined. Open circles show L-glucose uptake. A time course of D-glucose uptake (open squares) taken at 5-s intervals over a period of 15 s is shown for comparative purposes.

**Nonlinear regression analysis supports a model of a multiple-carrier transport system.** YPH500 was grown to mid-log phase and shifted to either repressing (2% glucose) or derepressing (0.05% glucose) conditions for 2 h. Cells were subse-

quently assayed for glucose uptake assay activity, and the resultant data were then used for computer-assisted nonlinear regression analysis (Fig. 2). The same data sets are presented in Michaelis-Menten and Lineweaver-Burk forms to demonstrate the degree of correlation of the model to the data at the different extremes of substrate concentration. The Eadie-Hofstee plot has traditionally been used for display of such data and is given as a reference for comparison with other such plots. The kinetic constants obtained in this way and their coefficients of correlation to the experimental data are presented in Table 1. The data presented indicate that glucose uptake kinetics in *S. cerevisiae* are consistent with a multiple-component system.

Attempts to model these same data by using the method and assumptions of Fuhrmann et al. (12–14, 39) are displayed in Fig. 2, and the values of the constants are displayed in Table 1; here, uptake is described as the resulting from the activity of a single carrier and free diffusion (equation 3). The constants given in Table 1 were generated so as to fit a Michaelis-Menten plot (Fig. 2d), as was the case in the reports referenced above. Attempts to generate constants that describe all three plots

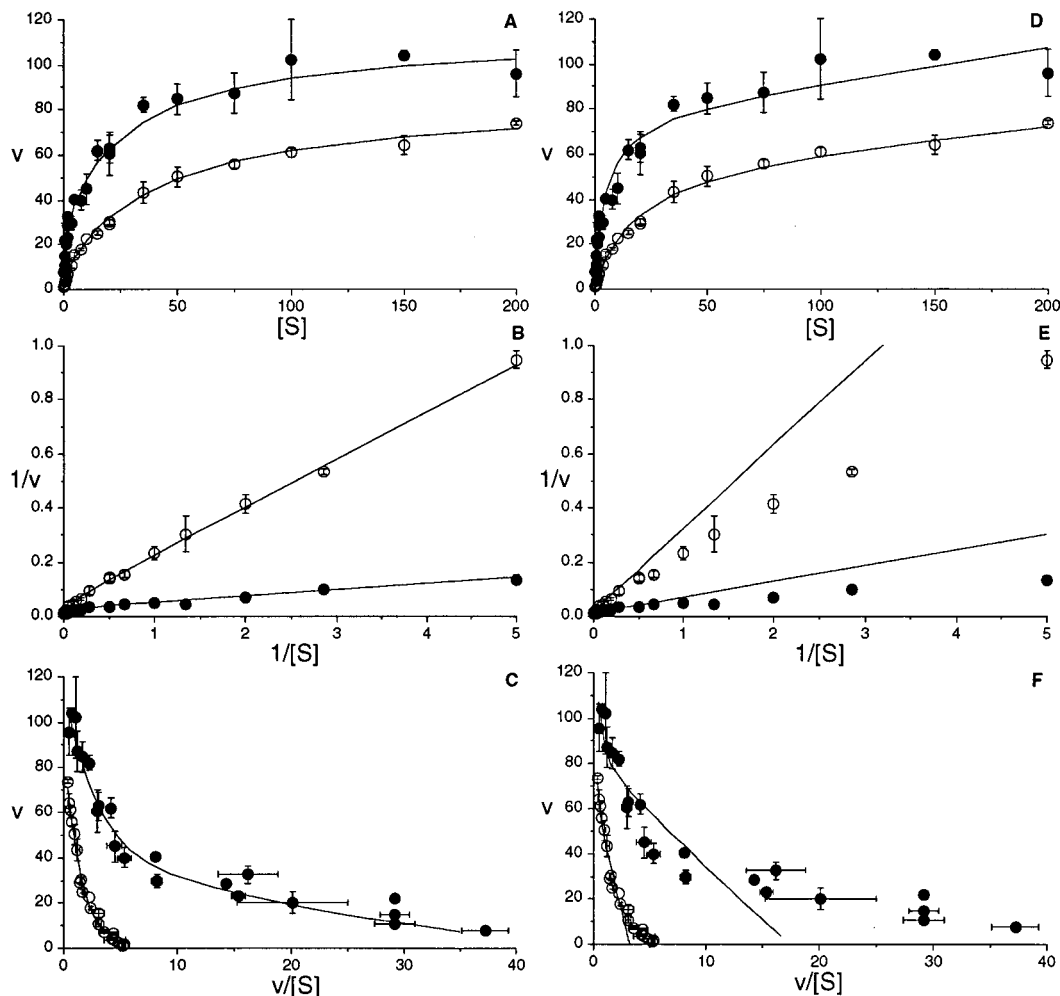


FIG. 2. Graphic representation of D-glucose uptake kinetics in wild-type yeast cells. D-Glucose uptake in YPH500 is shown by using three different graphic forms and two different kinetic models. Experimental data are shown as open circles for repressing conditions (2% glucose) and filled circles for derepressing conditions (0.05% glucose). The kinetic plots predicted by computer-assisted nonlinear regression analysis are shown as solid lines. The corresponding kinetic constants are given in Table 1. Panels A to C show predicted plots based on a two-carrier model; panels D to F show predicted plots based on a model of one saturable and one nonsaturable component. Velocity ( $v$ ) is expressed as nanomoles per minute per milligram (dry weight);  $[S]$  is the glucose concentration in millimolarity.

TABLE 1. Kinetic constants describing uptake of D-glucose by *S. cerevisiae* under repressing and derepressing conditions<sup>a</sup>

Glucose level	Reference figure	$K_{m1}$ (mM)	$V_{max1}$ (nmol/min/mg [dry wt])	$K_{m2}$ (mM)	$V_{max2}$ (nmol/min/mg [dry wt])	$R^2$		Reference figure	$K_m$ (mM)	$V_{max}$ (nmol/min/mg [dry wt])	$K_d$ ( $\mu$ l/mg/min)	$r^2$	
						Michaelis-Menten	Lineweaver-Burk					Michaelis-Menten	Lineweaver-Burk
Low	2A-C	27.64 (3.55)	84.83 (3.82)	0.67 (0.07)	29.08 (1.95)	0.9957	0.9948	2D-F	4.61 (1.14)	79.18 (6.95)	0.15 (0.05)	0.9863	0.1428
	2A-C	43.4 (2.85)	76.76 (1.92)	2.15 (0.23)	8.54 (0.77)	0.9983	0.9992	2D-F	19.18 (2.73)	60.51 (4.87)	0.09 (0.02)	0.9974	0.6337
High													

<sup>a</sup> Kinetic constants were derived from experimental data (shown in Fig. 2) by using computer-assisted nonlinear regression analysis. For the two-carrier model, the values given best describe both the Michaelis-Menten and the Lineweaver-Burk plots. For the one carrier-plus-diffusion model, the constants given best describe only the Michaelis-Menten plot. The values given in parentheses are the standard deviations ( $\sigma$ ) of the estimations. The derived kinetic constants are given to two decimal places to best describe the line generated, not to reflect the degree of accuracy of the values. The margin of experimental error precludes determination of the values to that fine of a degree. The coefficients of correlation ( $R^2$ ) values show the degree of correlation of the line generated by using these constants and the appropriate equation to the experimental data plotted in the form noted.

with a high degree of correlation, as was done for the two-carrier model, were not successful. It is apparent both from the plots and from the values of the correlation coefficients that a model of uptake as a combination of a single carrier and free diffusion cannot adequately describe the observed rates. In particular, by using the Michaelis-Menten plot to model the data, the contribution of the high-affinity component is underestimated. A similar phenomenon is observed if one compares the constants quoted by Fuhrmann et al. (12-14, 39) with the experimental data plotted in either an Eadie-Hofstee or Lineweaver-Burk form. It should also be noted that the uptake rates quoted by Wrede et al. (39), which were derived from data of Kruckeberg and Bisson (20) and subsequently used for computer-assisted nonlinear regression analysis, are not the same as those reported by Kruckeberg and Bisson (20) and that the analysis of those does not reflect the transport activity in *hxt2* null or wild-type strains.

**Inhibition kinetics are consistent with the presence of multiple carriers.** Genetic and biochemical data suggest that both 2-DOG and fructose are alternative substrates for at least some of the putative yeast hexose permeases (3). Glucose uptake was monitored in the presence of different concentrations of these compounds, and the results were compared with rates obtained without an inhibitor (Fig. 3 and 4). These graphs were then subjected to regression analysis (Tables 2 and 3).

It is apparent that the high-affinity component is severely inhibited at 2-DOG concentrations of 50 and 100 mM and with 100 mM fructose. Indeed, the degree of inhibition is so great that it makes accurate determination of kinetic constants describing this system at these concentrations difficult. The values returned by the regression program reflect this problem and must be interpreted accordingly. Nearly the entire high-affinity system's contribution to uptake is eliminated at these concentrations of inhibitor. Analysis of inhibition of uptake by 1 mM fructose reveals that neither system is significantly affected at that concentration. However, the kinetic constants describing transport in the presence of 10 mM fructose indicate inhibition of high-affinity, but not low-affinity, uptake.

2-DOG is also inhibitory to the low-affinity uptake system. The increase in the estimated  $K_m$  value for the low-affinity uptake system, relative to the value obtained without an inhibitor, indicates that 100 mM 2-DOG acts as a competitive inhibitor of this system. Were low-affinity uptake actually simple diffusion, inhibition would not be predicted or observed. Fructose at 100 mM seems to inhibit low-affinity uptake, though the effect is manifested primarily as a reduction in the  $V_{max}$  term, not as an increase in  $K_m$ . This  $V_{max}$  effect may result from noncompetitive inhibition of the transporter mediating low-affinity uptake or could result from competitive inhibition of a subset of the transporters mediating low-affinity uptake and noncompetitive inhibition of other transporters. Both compounds tested are capable of inhibition of both putative uptake systems. The inhibition patterns observed are consistent with a multicomponent uptake system.

***snf3* null mutants show reduced high-affinity uptake.** The kinetics of glucose uptake in the *snf3* null mutant strain LBY312 are shown in Fig. 5, and the results of regression analysis are given in Table 4. Consistent with earlier findings, this strain shows nearly wild-type levels of transport when grown in media containing 2% glucose. The kinetic constants indicate small differences in rate and affinity between LBY312 and YPH500 under these conditions, and the standard deviations of the low-affinity  $V_{max}$  and  $K_m$  indicate that these differences are significant. This finding may indicate that there is an effect of *snf3* deletion on cells grown in high glucose concentrations.

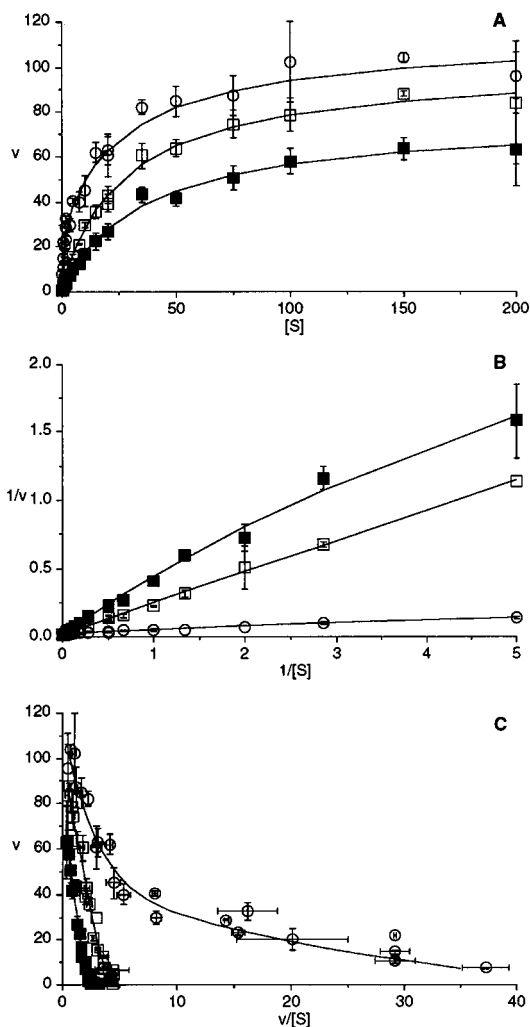


FIG. 3. Inhibition of glucose uptake kinetics by 2-DOG. Glucose uptake in YPH500 in the presence of 2-DOG is shown in three different graphic forms. Inhibitor concentrations were as follows: open circles, no 2-DOG (same data set as for 0.05% glucose in Fig. 2); open squares, 50 mM 2-DOG; closed squares, 100 mM 2-DOG. The kinetic plots predicted by computer-assisted nonlinear regression analysis are shown as solid lines. Only the model plots for two-carrier inhibition are presented; the plots for high-affinity-only inhibition are indistinguishable from the former. The corresponding kinetic constants are given in Table 2.

The plots and regression analysis both indicate that there seems to be a reduction, not a complete elimination, of the high-affinity component upon a shift to derepressing conditions. Further, there seems to be a subtle effect of *snf3* deletion on low-affinity transport in cells grown in low glucose as well. This was not observed previously (7).

## DISCUSSION

An iterative, nonlinear regression analysis of alternative transformations has been used to model the observed kinetics of glucose uptake in *S. cerevisiae* and is consistent with a multiple-carrier-mediated system, in support of the observation of a multigene family of glucose transporters. Using an improved uptake assay and analysis, we show that diffusion does not significantly contribute to uptake and that the kinetics are consistent with a two-carrier-mediated system. It has been sug-

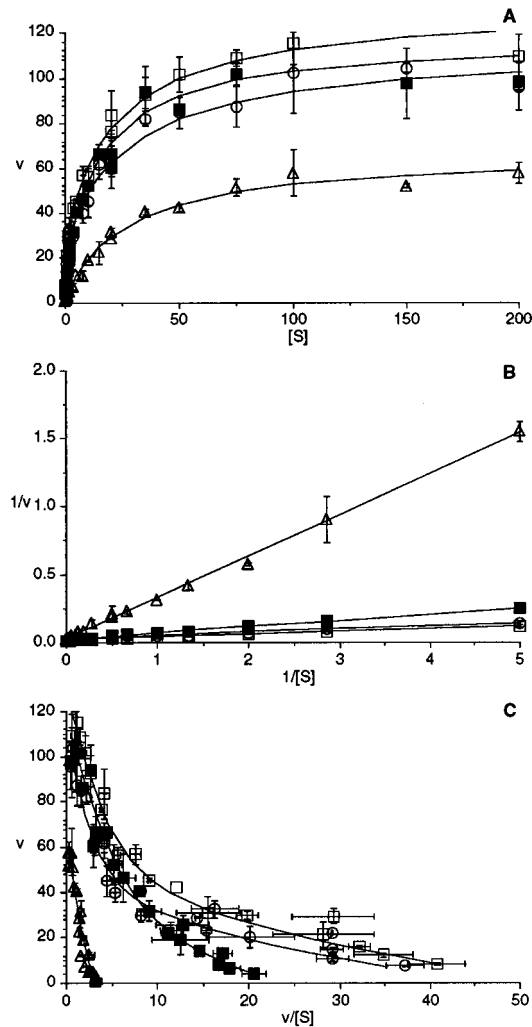


FIG. 4. Inhibition of glucose uptake kinetics by fructose. Glucose uptake in YPH500 in the presence of fructose is shown in three different graphic forms. Inhibitor concentrations were as follows: open circles, no fructose (same data set as for 0.05% glucose in Fig. 2); open squares, 1 mM fructose; closed squares, 10 mM fructose; open triangles, 100 mM fructose. The kinetic plots predicted by computer-assisted nonlinear regression analysis are shown as solid lines. Only the model plots for two-carrier inhibition are presented; the plots for high-affinity-only inhibition are indistinguishable from the former. The corresponding kinetic constants are given in Table 3.

gested that there are not two systems but rather a single system with a constant  $V_{\max}$  value and a  $K_m$  that varies in response to growth state (35). In our analysis,  $V_{\max}$  was not constant, a finding consistent with known regulatory properties of the *HXT* genes (19, 23, 33, 36, 37). However, it should be stressed

TABLE 2. Kinetic constants describing uptake of D-glucose in the presence of 2-deoxyglucose<sup>a</sup>

2-DOG concn (mM)	$K_{m1}$ (mM)	$V_{\max 1}$ (nmol/min/mg [dry wt])	$K_{m2}$ (mM)	$V_{\max 2}$ (nmol/min/mg [dry wt])	$r^2$	
					Michaelis-Menten	Lineweaver-Burk
50	27.1	98.29	1.61	1.38	0.9983	0.9990
100	35.32	75.89	0	0.1927	0.9975	0.9970

<sup>a</sup> Data are from Fig. 3. For other details, see the footnote to Table 1.

TABLE 3. Kinetic constants describing uptake of D-glucose in the presence of fructose<sup>a</sup>

Fructose concn (mM)	$K_{m1}$ (mM)	$V_{max1}$ (nmol/min/mg [dry wt])	$K_{m2}$ (mM)	$V_{max2}$ (nmol/min/mg [dry wt])	$r^2$	
					Michaelis-Menten	Line-weaver-Burk
1	21.65	99.21	0.65	30.76	0.9959	0.9933
10	16.96	99.09	1.081	18.44	0.9891	0.9984
100	29.92	61.45	4.59	5.55	0.9952	0.9983

<sup>a</sup> Data are from Fig. 4. For other details, see the footnote to Table 1.

TABLE 4. Kinetic constants describing uptake of D-glucose in the *snf3* null strain in the two-carrier model<sup>a</sup>

Glucose level	$K_{m1}$ (mM)	$V_{max1}$ (nmol/min/mg [dry wt])	$K_{m2}$ (mM)	$V_{max2}$ (nmol/min/mg [dry wt])	$r^2$	
					Michaelis-Menten	Line-weaver-Burk
Low	41.69	36.19	1.89	25.67	0.9968	0.9993
High	33.59	59.03	3.07	10.28	0.9994	0.9996

<sup>a</sup> Data are from Fig. 5. For other details, see the legend to Table 1.

that neither the findings discussed here nor those in previous papers (1–7, 20, 23, 26) can preclude the involvement of more systems than the two postulated. Genetic evidence suggests that these constants reflect, in fact, average values for a pop-

ulation of proteins active at the same time (3). That this population can be modeled as a two-carrier system is entirely consistent with our understanding of regression analysis (17, 18). Further elucidation of this process will likely result from close coordination of kinetic studies with the traditional approaches of cell biology and genetics. Kinetic analysis of wild-type and mutant strains under different growing conditions promise to give important insights into this complicated process.

Regression analysis of uptake under derepressing conditions results in kinetic constants remarkably close to those previously estimated from Eadie-Hofstee plots of similar data (4–6), and these findings are consistent with the model of a glucose-repressible component of transport activity postulated in those papers. However, as a result of more refined methods of estimation, the constants generated from repressing conditions differ somewhat from those presented previously (4–6) and may indicate that the current model of a constitutive low-affinity component is overly simplistic. That at least two carriers are needed to adequately describe these data indicates that a model of a single carrier is not correct. Rather, it appears that there are multiple proteins active under these conditions, with activities and substrate affinities apparently lower than those evidenced under derepressing conditions. Whether there are proteins common to both conditions and whether such proteins show altered activity in response to changing growth conditions is not clear, since HXT4 seems to affect both low- and high-affinity transport (33). Because of the complexity of the system and the limitations of regression analysis, it may be that uptake under derepressing conditions cannot be described as a sum of a constitutive low-affinity component and a repressed high-affinity component. Instead, it seems as though both components may undergo changes. That low-affinity transport might be regulated is not surprising in light of the number of regulatory cascades that affect uptake activity (3) and the apparent complex level of regulation of the *HXT* genes. Low-affinity transport does decrease in stationary phase, indicating at least one type of regulation (6).

Inhibition studies also indicate that at least two distinct uptake systems function during growth on low concentrations of glucose. The use of compounds thought to be alternative substrates of both systems shows that high-affinity uptake is inhibited by both compounds, whereas low-affinity uptake demonstrates competitive inhibition by 100 mM 2-DOG but what appears to be noncompetitive inhibition by 100 mM fructose. This apparent anomaly can be explained by a model of transport mediated by a population comprising a system of low-affinity hexose permeases of differing specificities, some of which are competitively inhibited by fructose while others are not. This would result in a  $V_{max}$  effect such as is observed. This model is consistent with what we know of the possible substrates for the identified *HXT* gene products (3).

Analysis of a *snf3* null strain reveals that the *SNF3* gene

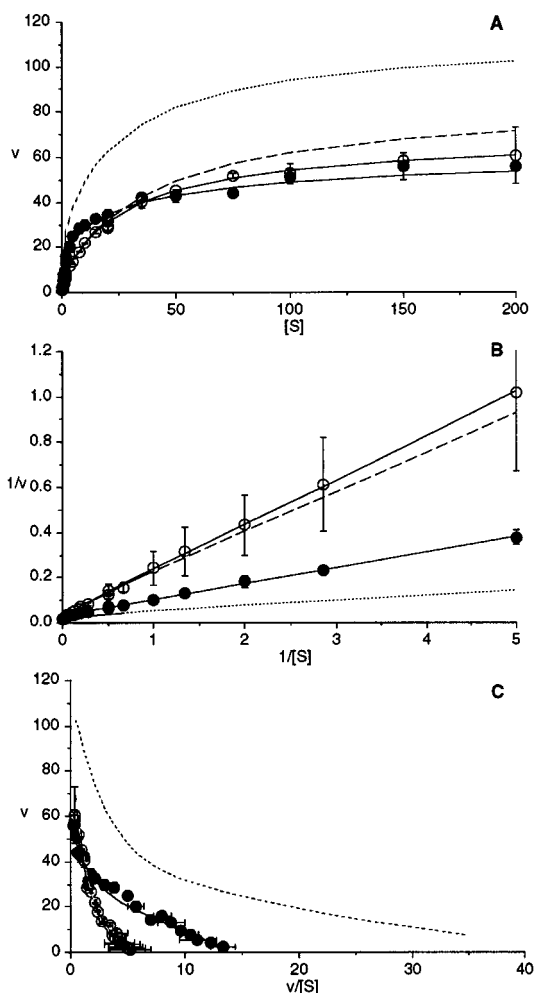


FIG. 5. Graphic representation of D-glucose uptake kinetics in *snf3* null yeast cells. D-Glucose uptake in LB312 is shown in three different graphic forms. Experimental data are shown as open circles for derepressing conditions (2% glucose) and filled circles for repressing conditions (0.05% glucose). The kinetic plots predicted by computer-assisted nonlinear regression analysis based on a two-carrier model are shown as solid lines. The corresponding kinetic constants are given in Table 4. Uptake activity in the wild type is shown for reference purposes. The best fits of the plots for YPH500 under derepressing (0.05% glucose) and repressing (2% glucose) conditions are shown as dotted and dashed lines, respectively.

product is mainly active under conditions of glucose limitation, as previously reported (9). While there may be some effect of *snf3* deletion on uptake kinetics under repressing conditions, it is minor and would be difficult to quantify or characterize at this time. These findings are consistent with what is known of the timing and conditions of *SNF3* expression from promoter-reporter gene fusions and from Northern (RNA) analysis (9; unpublished observations), which suggest that the *SNF3* promoter is glucose responsive.

It is interesting that the strain carrying the *snf3Δ::TRP1* allele used in this study exhibits slightly different transport kinetics than the strain carrying the *snf3Δ::HIS3* allele used previously (7, 20, 23, 25). This may be due to the presence of a wild-type *TRP1* locus, which may serve to alleviate a cryptic auxotrophic lesion in this background and allow improved growth. It could also be a result of the absence of the integrated *HIS3* gene. In other words, if the *HIS3* integrant is only partially able to complement, provision of histidine in the medium would lead to better growth.

#### ACKNOWLEDGMENTS

We thank Irwin Segel for his critique of and help in modification of the uptake assay and for his advice regarding the regression analysis.

This work was funded by U.S. Department of Agriculture grant 93-37308-9085 to Linda F. Bisson.

#### REFERENCES

- Bisson, L. F. 1988. Derepression of high-affinity glucose uptake requires a functional secretory system in *Saccharomyces cerevisiae*. *J. Bacteriol.* **170**:2654–2658.
- Bisson, L. F. 1988. High-affinity glucose transport in *Saccharomyces cerevisiae* is under general glucose repression control. *J. Bacteriol.* **170**:4838–4845.
- Bisson, L. F., D. M. Coons, A. L. Kruckeberg, and D. A. Lewis. 1993. Yeast sugar transporters. *Crit. Rev. Biochem. Mol. Biol.* **28**:259–308.
- Bisson, L. F., and D. G. Fraenkel. 1983. Involvement of kinases in glucose and fructose uptake by *Saccharomyces cerevisiae*. *Proc. Natl. Acad. Sci. USA* **80**:1730–1734.
- Bisson, L. F., and D. G. Fraenkel. 1983. Transport of 6-deoxyglucose in *Saccharomyces cerevisiae*. *J. Bacteriol.* **155**:995–1000.
- Bisson, L. F., and D. G. Fraenkel. 1984. Expression of kinase-dependent glucose uptake in *Saccharomyces cerevisiae*. *J. Bacteriol.* **159**:1013–1017.
- Bisson, L. F., L. Neigeborn, M. Carlson, and D. G. Fraenkel. 1987. The *SNF3* gene is required for high-affinity glucose transport in *Saccharomyces cerevisiae*. *J. Bacteriol.* **169**:1656–1662.
- Burger, M., L. Hejmova, and A. Kleinzeller. 1959. Transport of some mono- and di-saccharides into yeast cells. *J. Physiol.* **71**:233–242.
- Celenza, J. L., L. Marshall-Carlson, and M. Carlson. 1988. The yeast *SNF3* gene encodes a glucose transporter homologous to the mammalian protein. *Proc. Natl. Acad. Sci. USA* **85**:2130–2134.
- Cirillo, V. P. 1968. Relationship between sugar structure and competition for the sugar transport system in bakers' yeast. *J. Bacteriol.* **95**:603–611.
- Elledge, S. J., and R. W. Davis. 1988. A family of versatile centromeric vectors designed for use in the sectoring-shuffle mutagenesis assay in *Saccharomyces cerevisiae*. *Gene* **70**:303–312.
- Fuhrmann, G. F., and B. Völker. 1992. Regulation of glucose transport in *Saccharomyces cerevisiae*. *J. Biotechnol.* **27**:1–15.
- Fuhrmann, G. F., and B. Völker. 1993. Misuse of graphical analysis in nonlinear sugar transport kinetics by Eadie-Hofstee plots. *Biochim. Biophys. Acta* **1145**:180–182.
- Fuhrmann, G. F., B. Völker, S. Sander, and M. Potthast. 1989. Kinetic analysis and simulation of glucose transport in plasma membrane vesicles of glucose-repressed and derepressed *Saccharomyces cerevisiae* cells. *Experientia* **45**:1018–1023.
- Gonçalves, T., and M. C. Loureiro-Dias. 1994. Aspects of glucose uptake in *Saccharomyces cerevisiae*. *J. Bacteriol.* **176**:1511–1513.
- Gould, G. W., and G. I. Bell. 1990. Facilitative glucose transporters: an expanding family. *Trends Biochem. Sci.* **15**:18–23.
- Klotz, I. M. 1982. Numbers of receptor sites from Scatchard graphs: facts and fantasies. *Science* **217**:1247–1249.
- Klotz, I. M. 1985. Estimation of number of receptor sites: a misconception. *Biopharm. Drug Dispos.* **6**:105–107. (Letter.)
- Ko, C. H., H. Liang, and R. F. Gaber. 1993. Roles of multiple glucose transporters in *Saccharomyces cerevisiae*. *Mol. Cell. Biol.* **13**:638–648.
- Kruckeberg, A. L., and L. F. Bisson. 1990. The *HXT2* gene of *Saccharomyces cerevisiae* is required for high affinity glucose transport. *Mol. Cell. Biol.* **10**:5903–5913.
- Lagunas, R. 1993. Sugar transport in *Saccharomyces cerevisiae*. *FEMS Microbiol. Rev.* **10**:229–242.
- Leatherbarrow, R. J. 1990. Using linear and non-linear regression to fit biochemical data. *Trends Biochem. Sci.* **15**:455–458.
- Lewis, D. A., and L. F. Bisson. 1991. The *HXT1* gene product of *Saccharomyces cerevisiae* is a new member of the family of hexose transporters. *Mol. Cell. Biol.* **11**:3804–3813.
- Lowe, A. G. 1989. Molecular aspects of sugar, nucleotide and sugar nucleotide transport. *Biochem. Soc. Transact.* **17**:435–438.
- Marshall-Carlson, L., L. Neigeborn, D. Coons, L. Bisson, and M. Carlson. 1991. Dominant and recessive suppressors that restore glucose transport in a yeast *snf3* mutant. *Genetics* **128**:505–512.
- McClellan, C. J., and L. F. Bisson. 1988. Glucose uptake in *Saccharomyces cerevisiae* grown under anaerobic conditions: effects of null mutations in the hexokinase and glucokinase structural genes. *J. Bacteriol.* **170**:5396–5400.
- Neigeborn, L., P. Schwartzberg, R. Reed, and M. Carlson. 1986. Null mutations in the *SNF3* gene of *Saccharomyces cerevisiae* cause a different phenotype than previously isolated missense mutations. *Mol. Cell. Biol.* **6**:3569–3574.
- Nishizawa, K. E., Shimoda, and M. Kashara. 1995. Substrate recognition domain of the Gal2 galactose transporter in yeast *Saccharomyces cerevisiae* as revealed by chimeric galactose-glucose transporters. *J. Biol. Chem.* **270**:2423–2426.
- Schena, M., D. Picard, and K. R. Yamamoto. 1991. Vectors for constitutive and inducible gene expression in yeast. *Methods Enzymol.* **194**:389–398.
- Schneider, R. P., and W. R. Wiley. 1971. Kinetic characteristics of the two glucose transport systems in *Neurospora crassa*. *J. Bacteriol.* **106**:479–486.
- Sen, A. K., and W. F. Widdas. 1962. Determination of the temperature and pH dependence of glucose transfer across the human erythrocyte membrane measured by glucose exit. *J. Physiol.* **160**:392–403.
- Sikorski, R. J., and P. Hieter. 1989. A system of shuttle vectors and host strains designed for efficient manipulation of DNA in *Saccharomyces cerevisiae*. *Genetics* **122**:19–27.
- Theodoris, G., N. M. Fong, D. M. Coons, and L. F. Bisson. 1994. High-copy suppression of glucose transport defects by *HXT4* and regulatory elements in the promoters of the *HXT* genes in *Saccharomyces cerevisiae*. *Genetics* **137**:957–966.
- Walmsley, A. R. 1988. The dynamics of the glucose transporter. *Trends Biochem. Sci.* **13**:226–231.
- Walsh, M. C., H. P. Smits, M. Scholte, and D. K. van. 1994. Affinity of glucose transport in *Saccharomyces cerevisiae* is modulated during growth on glucose. *J. Bacteriol.* **176**:953–958.
- Wendell, D. L., and L. F. Bisson. 1993. Physiological characterization of putative high-affinity glucose transport protein Hxt2 of *Saccharomyces cerevisiae* by use of anti-synthetic peptide antibodies. *J. Bacteriol.* **175**:7689–7696.
- Wendell, D. L., and L. F. Bisson. 1994. Expression of high-affinity glucose transport protein Hxt2p of *Saccharomyces cerevisiae* is both repressed and induced by glucose and appears to be regulated posttranslationally. *J. Bacteriol.* **176**:3730–3737.
- Widdas, W. F. 1988. Old and new concepts of the membrane transport for glucose in cells. *Biochim. Biophys. Acta* **947**:385–404.
- Wrede, C., B. Völker, H. Küntzel, and G. F. Fuhrmann. 1992. Kinetic analysis of glucose transport in wild-type and transporter deficient *Saccharomyces cerevisiae* strains under glucose repression and derepression. *J. Biotechnol.* **27**:47–57.